Applied Thermal Engineering 62 (2014) 13–19

Contents lists available at ScienceDirect

Applied Thermal Engineering

journal homepage: www.elsevier.com/locate/apthermeng

Effect of bluff body shape on the blow-off limit of hydrogen/air flame in a planar micro-combustor

Aiwu Fan*, Jianlong Wan, Yi Liu, Boming Pi, Hong Yao, Wei Liu

State Key Laboratory of Coal Combustion, Huazhong University of Science and Technology, 1037 Luoyu Road, Wuhan 430074, China

HIGHLIGHTS

- Effect of bluff body shape on blow-off limit of a micro-combustor was investigated.
- Blowout occurs due to flame stretching for triangular and semicircular bluff bodies.
- Triangular bluff body has a lower blow-off limit due to stronger flame stretching.
- Heat losses have a negligible effect on the difference of blow-off limit.

ARTICLE INFO

Article history:
Received 4 May 2013
Accepted 6 September 2013
Available online 19 September 2013

Keywords:
Micro-combustor
Bluff body
Blow-off limit
Recirculation zone
Flame stretching
Heat losses

ABSTRACT

We recently developed a micro-combustor with a triangular bluff body, which has a demonstrated 5-time extension in the blow-off limit compared to straight channel. In the present work, the effect of bluff body shape on the blow-off limit was investigated with a detailed H_2/air reaction mechanism. The results show that the blow-off limits for the triangular and semicircular bluff bodies are 36 and 43 m/s respectively at the same equivalence ratio of 0.5. Analyses reveal that flame blowout occurs due to the stretching effect in the shear layers for both the triangular and semicircular bluff bodies. Moreover, it is found that the triangular bluff body has a smaller blow-off limit because of the stronger flame stretching as compared with the semicircular case. Calculations indicate that the two cases have negligible differences in heat losses because the reaction zones and high temperature regions are located in the combustor centers. Therefore, the heat losses have a negligible effect on the difference in the blow-off limit of the two micro-combustors.

1. Introduction

With the rapid progresses of MEMS technology, various micro- and meso-scale devices and systems, such as micro propulsion systems, gas-turbines, robots, and portable electric devices, have continuously appeared [1,2]. As conventional batteries have disadvantages of low energy densities, short life spans and long recharging periods, the combustion-based micro-power generation devices are regarded as a potential alternative due to the much higher energy densities of hydrocarbon fuels [1,2]. The micro-combustor is a key component of micro-power generation systems. This component converts the chemical energy of fuels into thermal energy through combustion. Thus, the development of micro-combustors with a wide and stable operational range has attracted increasing attention over the last decade.

However, maintaining stable combustion in a micro-combustor is challenging. The increased heat loss and wall radical capture due to the large surface area-to-volume ratio make it difficult to sustain a stable flame at small scales [3,4]. Many unstable micro-flames have been reported to date [5–19]. For instance, Maruta et al. [5] experimentally observed a flame with repetitive extinction and ignition (FREI) in a 2-mm-diameter tube. Richecoeur and Kyritsis [6] identified the similar phenomenon in a 4-mm-diameter curved duct. This combustion mode was later numerically re-produced by other researchers [7–9]. After that, flame splitting phenomenon during the FREI processes was numerically predicted [10] and experimentally confirmed [11]. Additionally, Kumar et al. [12,13] and Fan et al. [14–19] observed some special flame patterns, such as the rotating spiral flame in a heated radial micro-channel.

Considerable efforts have been made to improve the flame stability in micro- and meso-scale combustors. Thermal managements, such as heat recirculation and heat loss control, are good ways to suppress the negative effect of heat losses and thus sustain a stable flame in small devices. The "Swill-roll" structure is a good

* Corresponding author. Tel.: +86 27 87542618; fax: +86 27 87540724.
E-mail addresses: faw@hust.edu.cn, faw_73@163.com (A. Fan).

1359-4311/$ – see front matter © 2013 Elsevier Ltd. All rights reserved.
http://dx.doi.org/10.1016/j.applthermaleng.2013.09.010

example of heat recirculation that has been implemented to stabilize flames in micro- and meso-scale combustors [20–22]. Combustion characteristics of premixed H_2/air in a planar micro-combustor with stainless steel mesh [23] or SiC porous media [24] were experimentally studied. It is shown that the flame can be effectively anchored by the inserted porous media. Jiang et al. [25] developed a miniature cylindrical combustor with a porous wall. The flame can be stabilized in the combustor chamber due to the reduction of heat losses and the preheating effect on the cold fresh mixture.

Utilizing the flow recirculation zone of the flow field is another effective way to stabilize flame in micro-combustors. For instance, Yang et al. [26] and Pan et al. [27] developed a micro-combustor with a backward facing step. The experimental results showed that this structure is useful to control the flame position and widen the operation ranges of inlet velocity and H_2/air ratio. Khandelwal et al. [28] investigated the flame stability of CH_4/air mixture in micro-combustors with two backward steps. They verified that stable flames exist in these micro-combustors for wide ranges of inlet velocity and equivalence ratio. Wu et al. [29] proposed a modified design of the micro-gas turbine originally developed by the MIT group [30]. They added an additional wafer to regulate the velocity distribution and direction near the combustor entrance. Their numerical results indicate that the improved design significantly extends the operating range of mass flow rate, which may lead to higher power density of the micro-combustor. Wan et al. [31] developed a micro-combustor with a triangular bluff body which can extend the blow-off limit by more than five times as compared with the straight channel. Very recently, Fan et al. [32,33] investigated the effects of the bluff body dimension and the solid material on the blow-off limit of this micro combustor. It is shown that the dimensionless size of the bluff body (called the blockage ratio and defined as $\zeta = W_2/W_1$) should be larger than 0.3 to achieve a good performance of flame stabilization [32]. Moreover, it is revealed that a solid material with relatively low thermal conductivity and emissivity is beneficial to obtain a large blow-off limit for the micro bluff body combustor [33]. In addition to the bluff body dimension and the solid material, the geometric shape of the bluff body would also significantly influence the characteristics of the flow field and thus the flame stabilization ability in the micro-combustor. Therefore, in the present work, we are dedicated to investigating the effect of bluff body shape on the blow-off limit of a lean H_2/air flame. The results are analyzed in terms of the flow field near the bluff body and heat losses from the outer walls of the combustor.

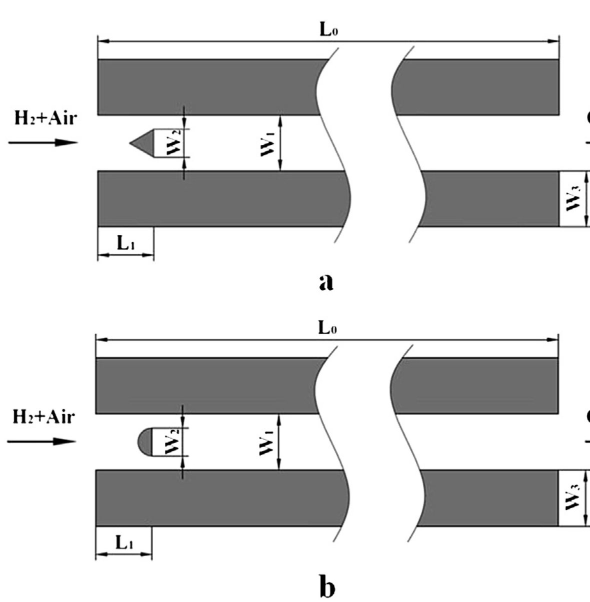

Fig. 1. Schematic diagram of the vertical cross sections of micro-combustors with a bluff body of different shapes: (a) equilateral triangle, (b) semicircle.

2. Numerical simulation method

2.1. Geometrical model

The schematic diagram of micro-combustors with a bluff body of different cross-sections, i.e., equilateral triangle and semicircle, is depicted in Fig. 1. The total length (L_0) and height (W_1) of the combustor chambers are 16.0 mm and 1.0 mm, respectively. The thickness of combustor walls (W_3) is 1.0 mm. The side lengths of the triangle (W_2) and the diameter of the semicircle (W_2) are the same of 0.5 mm. The bluff body is symmetrically located with respect to the upper and lower walls of the micro-combustor. The width of the bluff bodies is the same as that of the combustor chamber. The distance from the vertical surfaces of the triangle and semicircle to the combustor entrance (L_1) is 1.0 mm.

2.2. Mathematical model

As the characteristic length of the combustor chamber is still sufficiently larger than the molecular mean-free path of gases flowing through the micro-combustor, fluids can be reasonably considered as continuums and the Navier–Stokes equations are still suitable in the present study [34]. On the other hand, the mixing of various kinds of species is enhanced due to the small space and large concentration gradients in the micro-combustor. Therefore, turbulence models are expected to be better than the laminar model in reflecting the enhanced mixing and its effect on combustion characteristics. This has been confirmed by some researchers [21,31,35]. For example, Zhang et al. [35] reported that the turbulence model can get a much better prediction than the laminar model as compared with their experimental data. Kuo and Ronney [21] also suggest that it is more appropriate to predict the combustion characteristics in micro-combustors by using a turbulence model when the Reynolds number is larger than 500. In our case, the corresponding inlet velocity for Re = 500 is about 8.0 m/s. As the main purpose of the micro bluff body combustor is to extend the blow-off limit, which is larger than 8.0 m/s for H_2/air mixture at the equivalence ratio of 0.5 (refer to subsection 3.2). Besides, in our previous work [31], the predicted blow-off limit adopting the realizable k–epsilon turbulence model showed a reasonable agreement with experimental data. Therefore, we use the same model in the present paper. As heat conduction in the solid wall might affect the combustion significantly, the heat transfer in both of the combustor walls and the bluff body is considered in the present computation.

2.3. Computation scheme

Hydrogen and air are selected as fuel and oxidant, respectively. Quartz is used as the solid material. The detailed reaction mechanism reported by Li et al. [36] is applied to model the combustion of H_2/air mixtures. It consists of 13 species and 19 reversible elementary reactions. The surface reaction effect is not considered in CFD simulation because the micro-combustors could be processed via special measures which make the surfaces inert [37]. The thermodynamic and transport properties of the gaseous species could be found in the CHEMKIN databases [38,39].

Uniform velocity and concentration distributions of H_2/air mixture are specified at the inlet of micro-combustor. The mixture equivalence ratio is fixed at 0.5 in all cases. The inlet temperature of fuel/air mixture is set at 300 K. At the combustor exit, Neumann conditions are imposed on. Surface to surface radiation between interior surfaces of the combustor is considered by applying the discrete ordinates (DO) model [21]. For the exterior walls, the heat loss to the surroundings is calculated through Eq. (1),

$$q = h(T_{w,o} - T_\infty) + \varepsilon\sigma\left(T_{w,o}^4 - T_\infty^4\right) \quad (1)$$

where h is the natural convection heat transfer coefficient which takes a constant value of 20 W/(m^2 K) [40], $T_{w,o}$ is the outer wall temperature and T_∞ is the ambient temperature (300 K), ε is the emissivity of the solid surface with a value of 0.92, and σ is the Stephan–Boltzmann constant with a value of 5.67×10^{-8} W/(m^2 K^4).

The commercial software package, FLUENT 6.3 [41] was utilized to solve all the governing equations. Because the width of the combustor prototype is 10 mm, the aspect ratio (height/width = 1/10) of the combustor chamber is very small and the two-dimension solver was selected to reduce the computation load. The second-order upwind scheme was applied for discretization and the "SIMPLE" algorithm was adopted for the pressure–velocity coupling. Grid-independence of the results was checked and a non-uniform square grid system was applied in the computation. The minimum Δx and Δy of the grid are 0.01 mm. The grid numbers for the micro-combustors with triangular and semicircular bluff body are 47,742 and 44,988, respectively. The convergence of CFD simulation was judged when residuals of all governing equations were smaller than 1.0×10^{-6}.

3. Results and discussion

3.1. Model validation

In our previous study [31], the present numerical model has been validated by the experimental data, as shown in Fig. 2. It can be seen from Fig. 2 that the predicted blow-off limits agree reasonably well with the counterparts of the experiment. The relative errors between the numerical and experimental results are 5.3%, 12.2% and 5.8% for the equivalence ratios of 0.4, 0.5 and 0.6, respectively. In addition, we compared the computed and measured exhaust gas temperatures at a moderate inlet velocity of 20 m/s. It is shown that the difference is only 34.24 K. These confirm the reasonable accuracy of the numerical model adopted in the present paper.

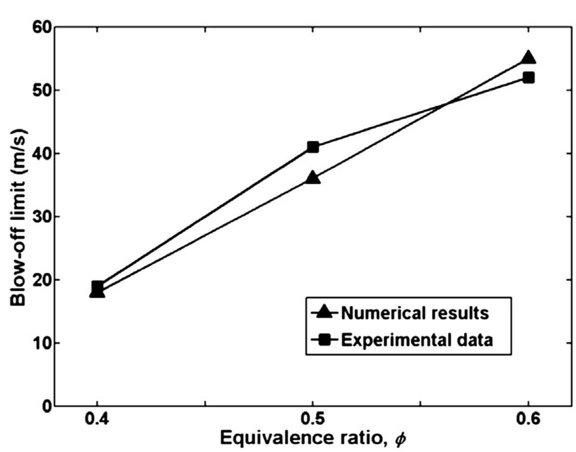

Fig. 2. Measured and predicted blow-off limits of the micro-combustor with a triangular bluff body [31].

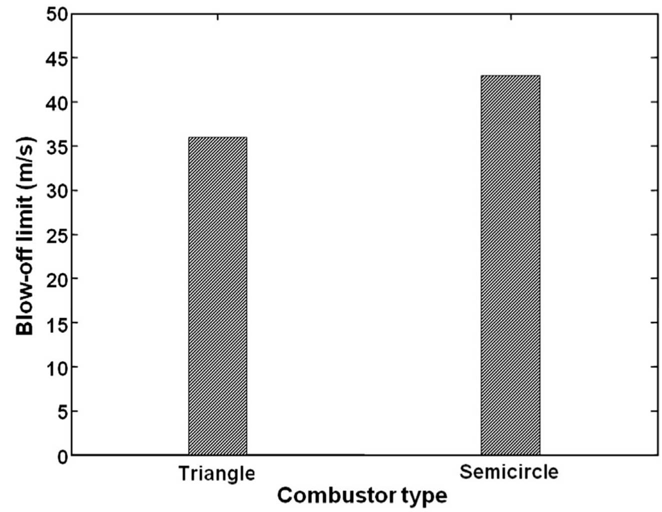

Fig. 3. The blow-off limit of the micro-combustor with a bluff body of different shapes.

3.2. Effect of bluff body shape on the blow-off limit

The blow-off limit of combustors with a bluff body of different shapes is shown in Fig. 3. It is seen from Fig. 3 that the corresponding blow-off limit for the triangular and semicircular bluff bodies is 36 and 43 m/s, respectively. In other words, the semicircular bluff body has a better flame stabilization ability than the triangular bluff body.

It is expected that the flame stabilization in the micro-combustor is affected by flow field, heat loss, etc. For the convenience of discussion, we here define a recirculation zone where the flow direction is opposite to the mainstream, i.e., the longitudinal velocity component V_x is less than zero (i.e., $V_x \le 0$) in this region. In addition, the heat loss ratio, Φ, is defined in Eq. (2) to indicate the proportion of heat loss from the outer walls, Q', to the input enthalpy involved in the fuel, Q.

$$\Phi = Q'/Q \quad (2)$$

3.3. Discussion

3.3.1. Flow field and reaction zone

It is well known that the recirculation zone has a dominated effect on the flame stabilization in the bluff body combustor. This is because the flow velocity in the recirculation zone is relatively low and a pool of key radicals (reaction zone) is formed. The size of the flame root (i.e., the part of flame that is located in the recirculation zone) is important for the stabilization of the whole flame. Therefore, the flame root can be anchored if the recirculation zone is sufficient large. Fig. 4 shows the contours of longitudinal velocity component in the vicinity of the bluff body ($x < 2.2$ mm) at the inlet velocity of 10 m/s. From Fig. 4, it is evident that the recirculation zones behind the triangular and semicircular bluff bodies are almost of the same size.

The recirculation zone exerts significant influence on the reaction zone which can be indicated by the high OH concentration region. In Fig. 5, the mass fraction contours of radical OH in the two combustors are shown. This figure depicts that the OH concentration in the downstream of the combustion chamber is higher for the case with a semicircle bluff body, which implies that the reaction zone area of this combustor is wider as compared with the combustor with triangular bluff body. For a clearer comparison between the reaction zones right behind the bluff bodies, the mass fraction contours of radical OH in the vicinity of the bluff body

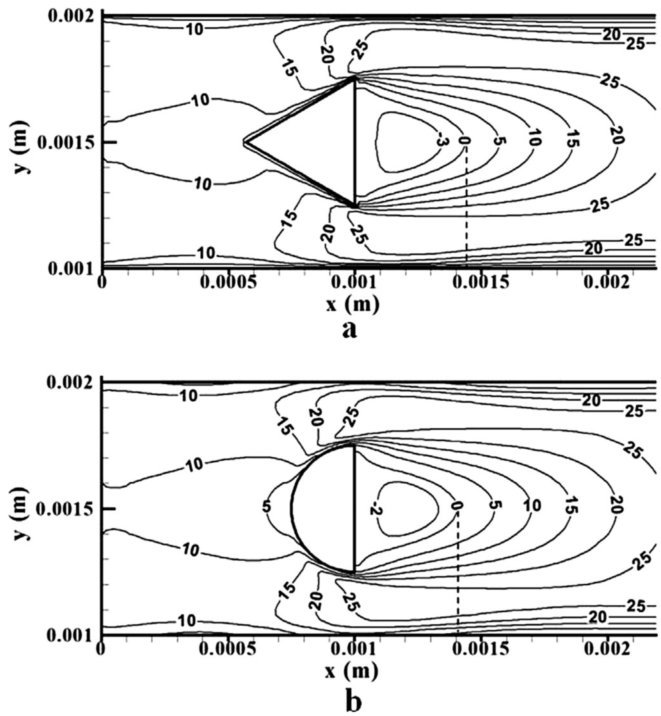

Fig. 4. Contours of the longitudinal velocity component near the bluff body ($x < 0.0022$ m) at the inlet velocity of 10 m/s: (a) equilateral triangle, (b) semicircle.

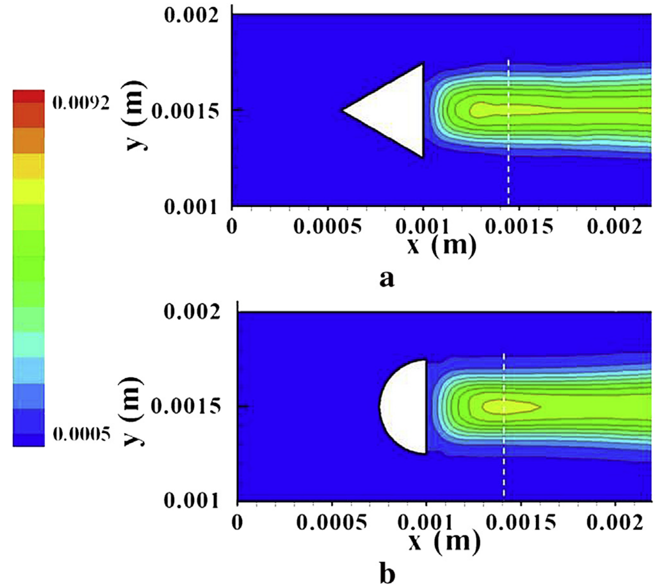

Fig. 6. Mass fraction contours of radical OH near the bluff body ($x < 0.0022$ m) at the inlet velocity of 10 m/s: (a) equilateral triangle, (b) semicircle.

($x < 2.2$ mm) are presented in Fig. 6, in which the right boundary of the recirculation zone is indicated by a dashed line. It is noted from Fig. 6 that the width of the reaction zone behind the semicircular bluff body is wider than that of the case with a triangular bluff body. This is helpful for the micro-combustor with a semicircular bluff body to obtain a comparatively higher blow-off limit.

In order to uncover the underlying mechanisms for the blowout of flame in the two cases, the reaction zones under blow-off limits are shown in Fig. 7. It is seen from Fig. 7 that the reaction zones behind the two bluff bodies are both prolonged and the whole reaction zones are almost splitted into two parts. The OH concentration in the recirculation zone is comparatively lower and the corresponding area is much narrower than the right part of the reaction zone. With a slightly further increase in the inlet velocity, the two parts of reaction zone will be totally separated and the flame can't sustain by solely depending on the smaller one in the recirculation zone. Consequently, the blowout of flame occurs. This phenomenon was also observed in our previous experimental investigation, as shown in Fig. 8. This photograph is directly taken with a digital camera under the blow-off limit condition of the micro-combustor with a triangular bluff body. From Fig. 8 it can also be seen that the flame is splitted before being blown out of the combustor.

The reason for the flame splitting is the stretching effect caused by the shear layers. To elucidate this, we present contours of the vertical velocity component near the bluff body in Fig. 9 and the locations of shear layers are roughly indicated by black arrows. It is clearly seen from Fig. 9 that the velocity gradient in the shear layers behind the triangular bluff body is comparatively larger than the counterpart of the case with a semicircular one. Therefore, the flame is more strongly stretched in the combustor with a triangular bluff body, which leads to a relatively smaller blow-off limit as compared with the case with a semicircular one.

3.3.2. Heat loss

Fig. 10 illustrates the outer wall temperature profiles of the two combustors at the inlet velocity of 10 m/s. It is noted from Fig. 10 that the two curves are almost overlapped. From the small figures embedded in Fig. 10, one can see that the upstream wall temperature of the combustor with a triangular bluff body is slightly lower

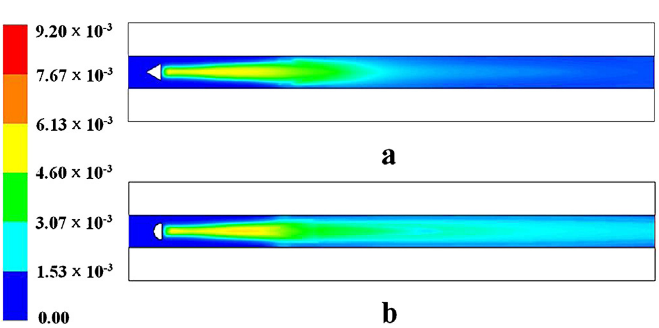

Fig. 5. Mass fraction contours of radical OH in the combustors at the inlet velocity of 10 m/s: (a) equilateral triangle, (b) semicircle.

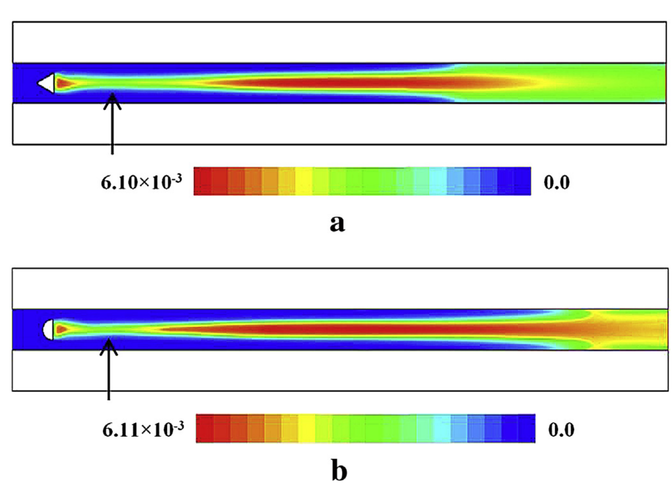

Fig. 7. Mass fraction contours of radical OH under the blow-off limits: (a) equilateral triangle, the blow-off limit is 36 m/s, (b) semicircle, the blow-off limit is 43 m/s.

Fig. 8. Flame photograph directly taken with a digital camera in our previous experiment under the blow-off limit of the micro-combustor with a triangular bluff body [32].

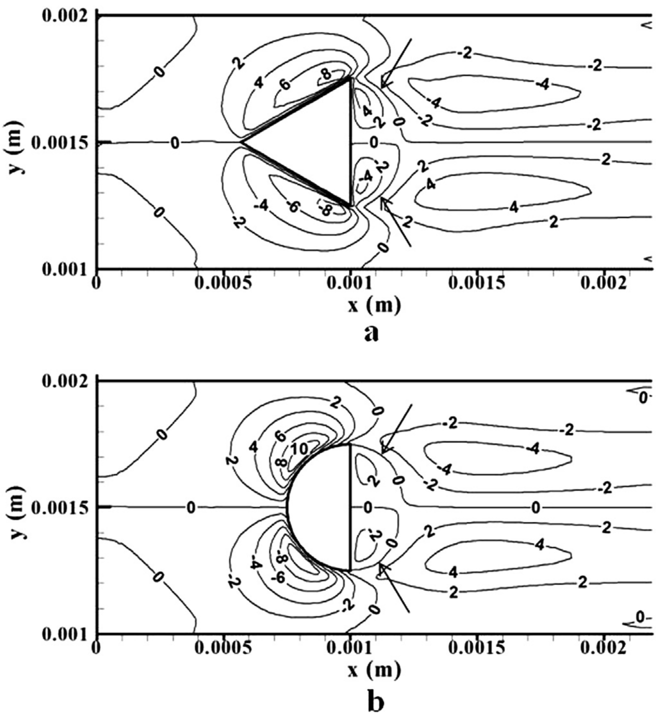

Fig. 9. Contours of the vertical velocity component near the bluff body ($x < 0.0022$ m) at the inlet velocity of 10 m/s: (a) equilateral triangle, (b) semicircle.

than that of the combustor with a semicircular bluff body, whereas its downstream wall temperature level is comparatively higher. For more details about the wall temperature profiles, we selected two points for comparison. For example, at the axial location of 3 mm, the outer wall temperatures for the micro-combustors with a triangular, and semicircular bluff body are 623 K and 640 K, respectively; while at the axial location of 11 mm, the outer wall temperatures for the micro-combustors with a circular, triangular, and semicircular bluff body are 1213 K and 1206 K, respectively. In

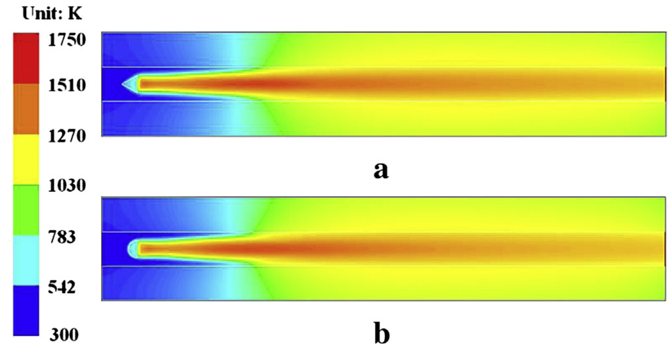

Fig. 11. Temperature fields of the combustors at the inlet velocity of 10 m/s: (a) equilateral triangle, (b) semicircle.

summary, the difference between outer wall temperature profiles of the two combustors is limited with a maximum of less than 20 K. The main reason is that, due to the existence of a bluff body, the reaction zone symmetrically locates in the center of the combustor chamber with respect to the upper and lower walls, which makes the high temperature zone also locate in the center of the combustor chamber, as shown in Fig. 11. As a result, the effect of the high temperature zone on combustor walls is negligible, and thus the differences between outer wall temperature profiles of the two cases are reduced.

Heat loss ratios (including convection heat loss ratio Φ_{con}, radiation heat loss ratio Φ_{rad}, and the total heat losses ratio Φ_{tot}) of the two combustors are calculated and presented in Fig. 12. The convection heat loss ratios of the two combustors are both 3.61%, and the radiation heat loss ratios for the combustor with triangular and semicircular bluff body are 19.59% and 19.42%, respectively. Therefore, the total heat-loss ratios for the combustor with triangular and semicircular bluff body are 23.20% and 23.03%, respectively. It is evident that the total heat loss ratio Φ_{tot} is dominated by the radiation mode Φ_{rad} and the heat loss component via convection Φ_{cov} is very small. This is because the wall temperatures levels of the two combustors are relatively high and emissivity of the quartz material is also very high (∼0.92). These data also reveals that the differences between the heat loss ratios of the two combustors are very limited, which indicates that it has a negligible effect on the differences of blow-off limits. We also calculated the combustion efficiency (also called chemical conversion efficiency), which is defined as

$$\eta_c = 1 - \frac{\text{Mass fraction of } H_2 \text{ at the exit}}{\text{Mass fraction of } H_2 \text{ at the inlet}} \quad (3)$$

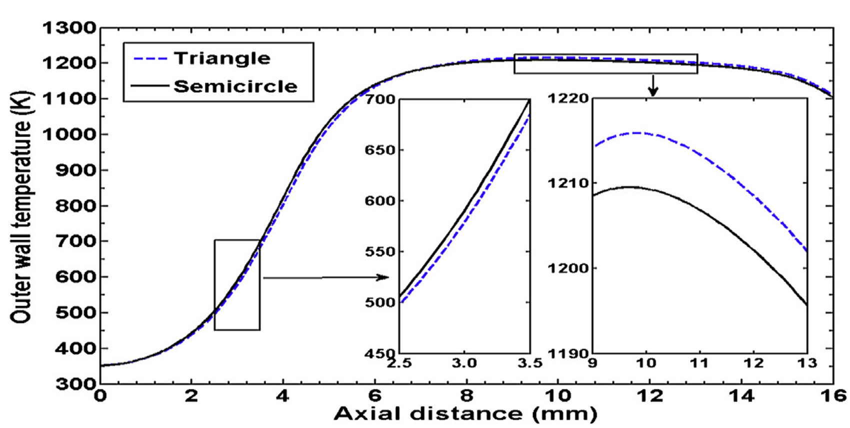

Fig. 10. Outer wall temperature profiles of the combustors with a bluff body of different shapes at the inlet velocity of 10 m/s.

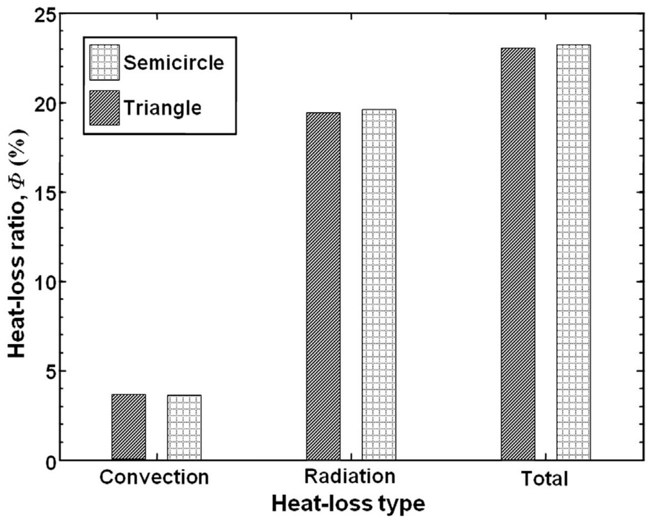

Fig. 12. Heat loss ratios of the combustors with a bluff body of different shapes.

It is found that the combustion efficiencies of the two micro-combustors are all above 99.0%. Therefore, it is not a main factor that affects the blow-off limit of the micro-combustor with a bluff body.

4. Conclusions

The effect of bluff body shape on the blow-off limit of a planar micro-combustor is numerically investigated with detailed H_2/air reaction mechanism. The results show that the blow-off limit of the combustor with a triangular and semicircular bluff body is around 36 and 43 m/s respectively at the equivalence ratio of 0.5. The reasons for the differences in blow-off limits are analyzed in terms of the recirculation zone and flame stretching as well as heat loss. It is demonstrated that the recirculation zones behind the triangular and semicircular bluff bodies are sufficient large and they are almost of the same size. However, for the combustor with a triangular bluff body, the flame stretching caused by the shear layers is comparatively stronger, which leads to a relatively smaller blow-off limit as compared with the semicircular bluff body. The analysis of heat loss reveals that it only has a negligible effect on the differences between blow-off limits of the two combustors with different bluff body shapes. Experimental investigations in the circular and semicircular bluff bodies will be carried out to further verify the predictions of the present work. These results will be reported in our future paper.

Acknowledgements

This work was supported by the Natural Science Foundation of China (Grant Nos. 51076054, 51276073, 51161140330 and 51076053) and the Foundation of Key Laboratory of Low-grade Energy Utilization Technologies and Systems, Chongqing University, China.

References

[1] A.C. Fernadez-pello, Micro-power generation using combustion: issues and approaches, Proc. Combust. Inst. 29 (2002) 883–899.
[2] K. Maruta, Micro and mesoscale combustion, Proc. Combust. Inst. 33 (2011) 125–150.
[3] J.W. Li, B.J. Zhong, Experimental investigation on heat loss and combustion in methane/oxygen micro-tube combustor, Appl. Therm. Eng. 28 (2008) 707–716.
[4] H.L. Yang, Y.X. Feng, X.H. Wang, L.Q. Jiang, D.Q. Zhao, N. Hayashi, H. Yamashita, OH-PLIF investigation of wall effects on the flame quenching in a slit burner, Proc. Combust. Inst. 34 (2013) 3379–3386.
[5] K. Maruta, T. Kataoka, N.I. Kim, S. Minaev, R. Fursenko, Characteristics of combustion in a narrow channel with a temperature gradient, Proc. Combust. Inst. 30 (2005) 2429–2436.
[6] F. Richecoeur, D.C. Kyritsis, Experimental study of flame stabilization in low Reynolds and Dean number flows in curved mesoscale ducts, Proc. Combust. Inst. 30 (2005) 2419–2427.
[7] T.L. Jackson, J. Buckmaster, Z. Lu, D.C. Kyritsis, L. Massa, Flames in narrow circular tubes, Proc. Combust. Inst. 31 (2007) 955–962.
[8] S. Minaev, K. Maruta, R. Fursenko, Nonlinear dynamics of flame in a narrow channel with a temperature gradient, Combust. Theory Modell. 11 (2007) 187–203.
[9] G. Pizza, C.E. Frouzakis, J. Mantzaras, A.G. Tomboulides, K. Boulouchos, Dynamics of premixed hydrogen/air flames in microchannels, Combust. Flame 152 (2008) 433–450.
[10] S. Minaev, E.V. Sereshchenko, R.V. Fursenko, A.W. Fan, K. Maruta, Splitting flames in a narrow channel with a temperature gradient in the walls, Combust. Explos. Shock Waves 45 (2009) 119–125.
[11] A.W. Fan, S. Minaev, E. Sereshchenko, Y. Tsuboi, H. Oshibe, H. Nakamura, K. Maruta, Dynamic behavior of splitting flames in a heated channel, Combust. Explos. Shock Waves 45 (2009) 245–250.
[12] S. Kumar, K. Maruta, S. Minaev, Pattern formation of flames in radial microchannels with lean methane–air mixtures, Phys. Rev. E 75 (2007) 016208.
[13] S. Kumar, K. Maruta, S. Minaev, On the formation of multiple rotating pelton-like flame structures in radial microchannels with lean methane–air mixtures, Proc. Combust. Inst. 31 (2007) 3261–3268.
[14] A.W. Fan, S. Minaev, S. Kumar, W. Liu, K. Maruta, Experimental study on flame pattern formation and combustion completeness in a radial micro-channel, J. Micromech. Microeng. 17 (2007) 2398–2406.
[15] A.W. Fan, S. Minaev, S. Kumar, W. Liu, K. Maruta, Regime diagrams and characteristics of flame patterns in radial microchannels with temperature gradients, Combust. Flame 153 (2008) 479–489.
[16] A.W. Fan, S. Minaev, E.V. Sereshchenko, R.V. Fursenko, S. Kumar, W. Liu, K. Maruta, Experimental and numerical investigations of flame pattern formation in a radial micro-channel, Proc. Combust. Inst. 32 (2009) 3059–3066.
[17] A.W. Fan, K. Maruta, H. Nakamura, S. Kumar, W. Liu, Experimental investigation on flame pattern formations of DME–air mixtures in a radial micro-channel, Combust. Flame 157 (2010) 1637–1642.
[18] A.W. Fan, H. Nakamura, K. Maruta, W. Liu, Experimental investigation of flame pattern transitions in a heated radial micro-channel, Appl. Therm. Eng. 47 (2012) 111–118.
[19] A.W. Fan, J.L. Wan, K. Maruta, H. Nakamura, H. Yao, W. Liu, Flame dynamics in a heated meso-scale radial channel, Proc. Combust. Inst. 34 (2013) 3351–3359.
[20] N.I. Kim, S. Aizumi, T. Yokomori, S. Kato, T. Fujimori, K. Maruta, Development and scale effects of small Swiss-roll combustors, Proc. Combust. Inst. 31 (2007) 3243–3250.
[21] C.H. Kuo, P.D. Ronney, Numerical modeling of non-adiabatic heat-recirculating combustors, Proc. Combust. Inst. 31 (2007) 3277–3284.
[22] B.J. Zhong, J.H. Wang, Experimental study on premixed CH_4/air mixture combustion in micro Swiss-roll combustors, Combust. Flame 157 (2010) 2222–2229.
[23] J. Li, S.K. Chou, Z.W. Li, W.M. Yang, Experimental investigation of porous media combustion in a planar micro-combustor, Fuel 89 (2010) 708–715.
[24] W.M. Yang, S.K. Chou, K.J. Chua, J. Li, X. Zhao, Research on modular micro combustor–radiator with and without porous media, Chem. Eng. J. 168 (2011) 799–802.
[25] L.Q. Jiang, D.Q. Zhao, X.H. Wang, W.B. Yang, Development of a self-thermal insulation miniature combustor, Energy Convers. Manage. 50 (2009) 1308–1313.
[26] W.M. Yang, S.K. Chou, C. Shu, Z.W. Li, H. Xue, Combustion in micro-cylindrical combustors with and without a backward facing step, Appl. Therm. Eng. 22 (2002) 1777–1787.
[27] J.F. Pan, J. Huang, D.T. Li, W.M. Yang, W.X. Tang, H. Xue, Effects of major parameters on micro-combustion for thermophotovoltaic energy conversion, Appl. Therm. Eng. 27 (2007) 1089–1095.
[28] B. Khandelwal, G.P.S. Sahota, S. Kumar, Investigations into the flame stability limits in a backward step micro scale combustor with premixed methane–air mixtures, J. Micromech. Microeng. 20 (2010) 095030.
[29] M. Wu, J. Hua, K. Kumar, An improved micro-combustor design for micro gas turbine engine and numerical analysis, J. Micromech. Microeng. 15 (2005) 1817–1823.
[30] A. Mehra, X. Zhang, A.A. Ayon, I.A. Waitz, M.A. Schmidt, C.M. Spadaccini, A six-wafer combustion system for a silicon micro gas turbine engine, J. Microelectromech. Syst. 9 (2000) 517–527.
[31] J.L. Wan, A.W. Fan, K. Maruta, H. Yao, W. Liu, Experimental and numerical investigation on combustion characteristics of premixed hydrogen/air flame in a micro-combustor with a bluff body, Int. J. Hydrogen Energy 37 (2012) 19190–19197.
[32] A.W. Fan, J.L. Wan, Yi Liu, B.M. Pi, H. Yao, K. Maruta, W. Liu, The effect of the blockage ratio on the blow-off limit of a hydrogen/air flame in a planar micro-combustor with a bluff body, Int. J. Hydrogen Energy 38 (2013) 11438–11445.

[33] A.W. Fan, J.L. Wan, K. Maruta, H. Yao, W. Liu, Interactions between heat transfer, flow field and flame stabilization in a micro-combustor with a bluff body, Int. J. Heat Mass Transfer 66 (2013) 72–79.
[34] A. Beskok, G.E. Karniadakis, A model for flows in channels, pipes, and ducts at micro and nano scales, Microscale Thermophys. Eng. 3 (1999) 43–77.
[35] Y.S. Zhang, J.H. Zhou, W.J. Yang, M.S. Liu, K.F. Cen, Study on the model selection for micro-combustion simulation, Proc. Chinese Soc. Electr. Eng. 26 (2006) 81–87 (in Chinese).
[36] J. Li, Z.W. Zhao, A. Kazakov, F.L. Dryer, An updated comprehensive kinetic model of hydrogen combustion, Int. J. Chem. Kinet. 36 (2004) 1–10.
[37] C.M. Miesse, R.I. Masel, M. Short, M.A. Shannon, Diffusion flame instabilities in a 0.75 mm non-premixed micro-burner, Proc. Combust. Inst. 30 (2005) 2499–2507.
[38] R.J. Kee, F.M. Rupley, J.A. Miller, The CHEMKIN Thermodynamic Database. Sandia National Laboratories Report SAND87-8215B, 1990.
[39] R.J. Kee, J.F. Grear, M.D. Smooke, J.A. Miller, A Fortran Program for Modeling Steady Laminar One-dimensional Premixed Flames. Sandia National Laboratories Report SAND 85-8240, 1985.
[40] J.P. Holman, Heat Transfer, ninth ed., McGraw-Hill, New York, 2002.
[41] Fluent 6.3 User's Guide, Fluent Inc., Lebanon, New Hampshire, 2006.